MedCrave
Step into the World of Research

Journal of Cancer Prevention & Current Research

Research Article

Open Access

CrossMark

Therapeutic potential of Pseudopterosin H on a prostate cancer cell line

Abstract

Metastatic castration resistant prostate cancer has remained predominantly incurable despite various advancements in cancer therapeutics. The lack of readily available and effective treatment options have driven research into alternative therapies, such as the use of marine natural products. Marine natural products are secondary metabolites produced by and isolated from marine organisms. A family of diterpene glycosides isolated from gorgonian soft corals, known as the Pseudopterosins, are of interest in cancer research. Previous studies performed on the Pseudopterosins have indicated that these compounds possess cytotoxic, anti-inflammatory, and anti-cancer activity in various malignant cell lines. We hypothesized that Pseudopterosin H will demonstrate anti-neoplastic activity in the PC-3 prostate cancer cell line by reducing cell viability and altering intracellular reactive oxygen species concentration through cytotoxic and apoptotic effects. Pseudopterosin H was isolated from the marine coral *Pseudopterogorgia elisabethae*. We assessed the therapeutic efficacy of Pseudopterosin H on the PC-3 cell line, at various treatment concentrations, through *in-vitro* assay screening using the MTT, NBT, and LDH assays, as well as AO/EB fluorescence. Results from our study have shown that treatment with Pseudopterosin H reduces PC-3 cell viability by inducing apoptosis and downregulating the production of intracellular reactive oxygen species. The chemosensitivity of PC-3 cells to treatment with Pseudopterosin H suggests the potential for prophylactic and therapeutic advantage in the treatment of metastatic castration resistant prostate cancer.

Volume 12 Issue 3 - 2021

Zoey Bowers,[1] Davian Caraballo,[1] Austin Bentley,[1] Toluleke Famuyiwa,[1] Joubin Jebelli,[1] James Kumi- Diaka,[1] Lyndon West[2]

[1]Department of Biological Sciences, Florida Atlantic University, USA

[2]Department of Chemistry and Biochemistry, Florida Atlantic University, USA

Correspondence: Zoey Bowers, Department of Biological Sciences, Florida Atlantic University, USA, Tel 239-699-0026, Email zbowes2016@fau.edu

Received: May 16, 2021 | **Published:** June 07, 2021

Introduction

Prostate cancer (PC) is the most commonly diagnosed male cancer and the second leading cause of male cancer deaths, in the United States.[1,2] It is expected that one in eight men will develop PC during their lifetime.[1] The 2021 U.S. estimates for PC diagnoses and deaths are 248,530 and 34,130, respectively.[1] Despite the United States' two decade long decrease in PC incidences, within the past decade (2008-2017) the percentage of incidences has remained relatively consistent.[1,2] The five-year clinical outcome of PC diagnoses is generally dependent on the characterization of the cancer as localized (non-metastasizing, contained within the prostate), regional (metastasis to structures or tissues surrounding the prostate), or distant (metastasis to organ(s) throughout the body, usually the bone).[3] Non-metastasizing PC has a five-year survival rate of approximately 98.9%, while metastasizing PC has a five-year survival rate of less than 30%.[4,5]

High five-year survival rates for non-metastasizing forms of PC are primarily attributed to the cellular response to androgens due to the expression of androgen receptors (AR).[4-7] AR is a ligand activated nuclear transcription factor that mediates the biological effects of androgens and is essential for normal prostate development and function.[5,8,9] However, androgens, AR ligands, have been shown to stimulate PC tumor cell proliferation and aid in tumorigenesis through the activation of secondary messengers and AR regulated genes.[9,10] Androgen deprivation therapy (ADT) is commonly used as a primary treatment for both metastasizing and non-metastasizing PC.[5-7] ADT includes drugs that inhibit androgen biosynthesis, such as Abiraterone, and AR blockers, such as Enzalutamide and Apalutamide.[5-7] ADT promotes tumor remission by inducing apoptosis in AR expressing prostate cells during androgen withdraw and is associated with the high five-year survival rates for non-metastasizing forms of PC.[5-7]

The progression from non-metastatic to metastatic PC can partially be attributed to the development of androgen resistance after the initial positive response of non-metastatic tumors to treatment with ADT.[5,8] Metastatic androgen resistant forms of PC are frequently referred to as metastatic castration resistant prostate cancer (mCRPC) and are correlated with a poor clinical prognosis.[4,5] The evolution of PC cells to androgen resistance (mCRPC) is currently unknown but may arise through AR driven mechanism(s) (i.e., AR overexpression and mutation), AR bypass mechanisms (i.e., glucocorticoid and progestogen receptors), or AR independent mechanisms (i.e., neuroendocrine differentiation and biological pathway coupling).[5] Additionally, less common variants of PC, such as small cell neuroendocrine carcinoma (SCNC), completely lack AR expression and therefore, do not have a response to ADT.[11] These clinical complications have caused a lack of effective treatment options for patients with castration resistant PC and mCRPC. Due to this, the discovery and development of alternative therapeutic options, such as the use of marine natural products, are critical for advancements in PC treatment and prevention.

Marine natural products (MNPs) are secondary metabolites produced by and isolated from marine organisms. Secondary metabolites originate from biological processes including, photosynthesis, glycolysis, the Krebs cycle, etc., and differ structurally and functionally from primary metabolites (carbohydrates, lipids, proteins, etc.).[12-14] Unlike primary metabolites, secondary metabolites are not required for homeostasis and, rather, they are often produced by the organism for defense through evolutionarily driven chemical modifications.[12-14] Over the last 50 years approximately 30,000 MNPs have been discovered, with approximately 75% of all discoveries originating from marine invertebrates.[12-14] Subsequently, these discoveries have resulted in six FDA approved marine derived drugs, four of which are used for treatment of various cancers: Cytarabine–acute myeloid leukemia, acute lymphocytic leukemia, chronic myelogenous leukemia, non-Hodgkin lymphoma; Eribulin Mesylate–metastatic breast cancer; Brentuximab Vedotin–Hodgkin's

lymphoma, systemic anaplastic large cell lymphoma; Trabectedin–soft tissue sarcoma.[12-13,15-21] The therapeutically advantageous properties of MNPs can be attributed to their biological origin and high affinity for binding to organic macromolecules (ex. cellular membrane receptors) as a result of their evolutionarily optimized nature.[12-14] Further, FDA approval of anti-cancer drugs originating from MNPs are expected to increase during the upcoming years. There are currently 20 new anti-cancer drugs of MNP origin in active FDA clinical trials and numerous other MNP compounds that exhibit anti-cancer potential in the beginning stages of research.[12,15,17]

Marine terpenes are the most biologically diverse class of MNPs. Terpenes are a promising source of compounds for anti-cancer drug development as terpenes and terpenoids make up 40.5% of MNPs that demonstrate anti-cancer activity.[22,23] A family of approximately 30 structurally related diterpene glycosides known as the Pseudopterosins, belong to this (terpene) class of marine compounds.[23-25] Pseudopterosins are isolated from gorgonian soft corals and each derivative possess a tricyclic diterpene core with a fucose or xylose moiety and differ in the degree of acetylation of the glycoside group as well as stereochemistry (C1 position can be alpha or beta).[23,26] These compounds are of interest for therapeutic use in various human diseases due to their diverse range of biological activities that include anti-inflammatory, analgesic, anti-microbial, anti-proliferative, wound healing, neuroprotective, and anti-cancer effects.[25,27-30] The known anti-inflammatory properties of Pseudopterosin compounds (hypothesized to occur via blocking the inflammatory pathway nuclear factor κB (NF-κB) through novel mechanisms of action), have resulted in their use in cosmetic skin care.[27-29] Further, the analgesic properties of these compounds have resulted in clinical trials for their potential as wound healing agents.[27-29] The anti-cancer effects of many of these compounds has remains vastly unexplored despite a handful of studies on Pseudopterosins (Ps) A-D, PsP, PsQ, PsS, PsT, PsU, 3-O-acetyl-PsU, seco-PsJ, and seco-PsU having demonstrated cytotoxic and anti-proliferative activity in various malignant cell lines (HeLa, cervical cancer; PC-3, prostate cancer; HCT116, colorectal cancer; MCF-7, breast cancer; BJ, fibroblasts; MDA-MB-231, breast cancer).[25,26,28,29] Additionally, to our knowledge, no studies have been published on the possible anti-cancer effects of Pseudopterosin H (PsH) on the PC-3 PC cell line.

In this study, the anti-cancer activity of PsH, isolated from the marine coral *Pseudopterogorgia elisabethae,* was assessed on the PC-3 PC cell line at various treatment concentrations. The PC-3 cell line was chosen as an *in-vitro* representation of mCRPC because of the lines vertebral metastasis origin and reported AR negativity.[7-9,11,31] The chemosensitivity of the PC-3 cells to treatment with PsH and potential mechanism(s) of action were determined through the use of various *in-vitro* assay screening techniques (MTT, LDH, NBT) and AO/EB fluorescence. Previous studies investigating the anti-cancer potential of structurally related Pseudopterosin compounds on a triple negative breast cancer cell line have concluded that these compounds possess cytotoxic and anti-cancer activity.[25,26,28,29] Therefore, due to the analogous nature of breast and prostate cancer, as well as the known anti-inflammatory effects of the Pseudopterosins, we hypothesize that treatment with Pseudopterosin H will reduce PC-3 cell viability by inducing apoptosis and altering the concentration of intracellular reactive oxygen species (ROS).

Results

Pseudopterosin H decreased PC-3 cell viability

Treatment with PsH decreased PC-3 cell viability in a concentration dependent manner (R^2=0.8160), relative to the negative control (0.000μM, 100%). PC-3 cell viability was significantly reduced at PsH treatment concentrations of 0.195μM, 0.390μM, and 1.560μM-100.000μM (Figure 1). PC-3 cell viability was reduced to less than 50% at PsH treatment concentrations of 25.000μM or greater (100.000μM, 19.25%; 50.000μM, 33.62%; 25.000μM, 39.41%) (Figure 1). The MTT assay data suggests that the IC_{50} value (half maximal inhibitory concentration; 50% metabolic function via oxidoreductase enzyme activity) of PsH on the PC-3 cell line is between 12.500μM and 25.000μM (Figure 1).

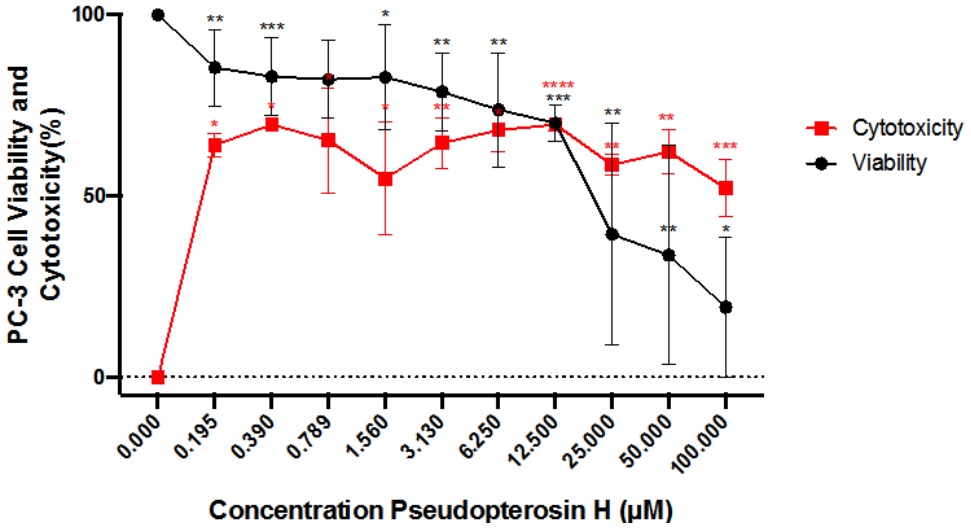

Figure 1 Percentage of PC-3 cell viability and cytotoxicity, relative to the negative control (0.000μM), after treatment with various concentrations of PsH (0.195μM-100.000μM). Treatment with PsH decreased the percentage of PC-3 cell viability in a concentration dependent manner (R^2=0.8160). PsH was significantly cytotoxic to PC-3 cells at all treatment concentrations (0.195μM-100.000μM) and cytotoxicity was independent of treatment concentration (R^2=0.0000250). Data points for PC-3 cell viability (MTT assay, black and oval-shaped legend) represent the mean values of four independent experiments (N=4 96-well plates; 8 total wells per treatment concentration, per plate). Data points for PC-3 cell cytotoxicity (LDH assay, red and square shaped legend) represent the mean values of two independent experiments (N=2 96-well plates; 8 total wells per treatment concentration, per plate). Error bars represent ± standard deviation of the means amongst all trials. Statistical significance is denoted by a single (*) asterisk when p<0.0332, double asterisks (**) when p<0.0021, triple asterisks (***) when p<0.0002, and quadruple asterisks (****) when p<0.00001.

Citation: Bowers Z, Caraballo D, Bentley A, et al. Therapeutic potential of Pseudopterosin H on a prostate cancer cell line. *J Cancer Prev Curr Res.* 2021;12(3):82–91. DOI: 10.15406/jcpcr.2021.12.00459

Pseudopterosin H caused a loss of PC-3 cellular membrane integrity

PsH was significantly cytotoxic to PC-3 cells at all treatment concentrations (0.195µM-100.000µM), relative to the negative control (0.000µM, 0%) (Figure 1). Treatment with the various concentrations of PsH (0.195µM-100.000µM) caused an approximate 50-70% increase in extracellular accumulation of lactate dehydrogenase (LDH) and therefore, increased loss of cellular membrane integrity, relative to that the negative control (0.000µM, 0%) (Figure 1). Additionally, the cytotoxic effects produced by treatment with PsH were independent of treatment concentration (R^2=0.0000250) (Figure 1).

Pseudopterosin H induced apoptosis in PC-3 cells

PsH treatment concentrations of 0.390µM-100.000µM produced a significant increase in the percentage of PC-3 cells undergoing apoptosis, relative to the negative control (0.000µM; Apoptosis, 8.215%) (Figure 2). The increasing percentage of PC-3 cells undergoing apoptosis was moderately dependent on PsH treatment concentration (R^2=0.6563) (Figure 2). PsH treatment concentrations of 0.390µM-100.000µM produced a significant decrease in live PC-3 cells, relative to the negative control (0.000µM; Live, 89.219%) (Figure 2). The decreasing percentage of live PC-3 cells was also moderately dependent on PsH treatment concentration (Figure 2). Necrotic cell death was minimally noted in the negative control (0.000µM, Necrosis, 4.805%) and in PsH treatment concentrations of 0.195µM-0.789µM (Necrosis, >1.750%) (Figure 2). Necrotic cell death was not observed in PC-3 cells treated with PsH at concentrations of 1.560µM–100.00µM (Figure 2). Necrosis was independent of PsH treatment concentration (R^2=0.06625) (Figure 2).

Pseudopterosin H downregulated intracellular ROS concentration in PC-3 cells

PsH significantly downregulated the percentage of intracellular reactive oxygen species (ROS) released by PC-3 cells at all treatment concentrations (0.195µM-100.000µM), relative to the negative control (0.000µM, 100%) (Figure 3). The percentage of ROS released by PC-3 cells was decreased by approximately 25-39% through treatment with PsH, relative to the negative control (0.000µM, 100%) (Figure 3). This decrease of ROS concentration in PC-3 cells was moderately dependent on PsH treatment concentration (R^2=0.677) (Figure 3).

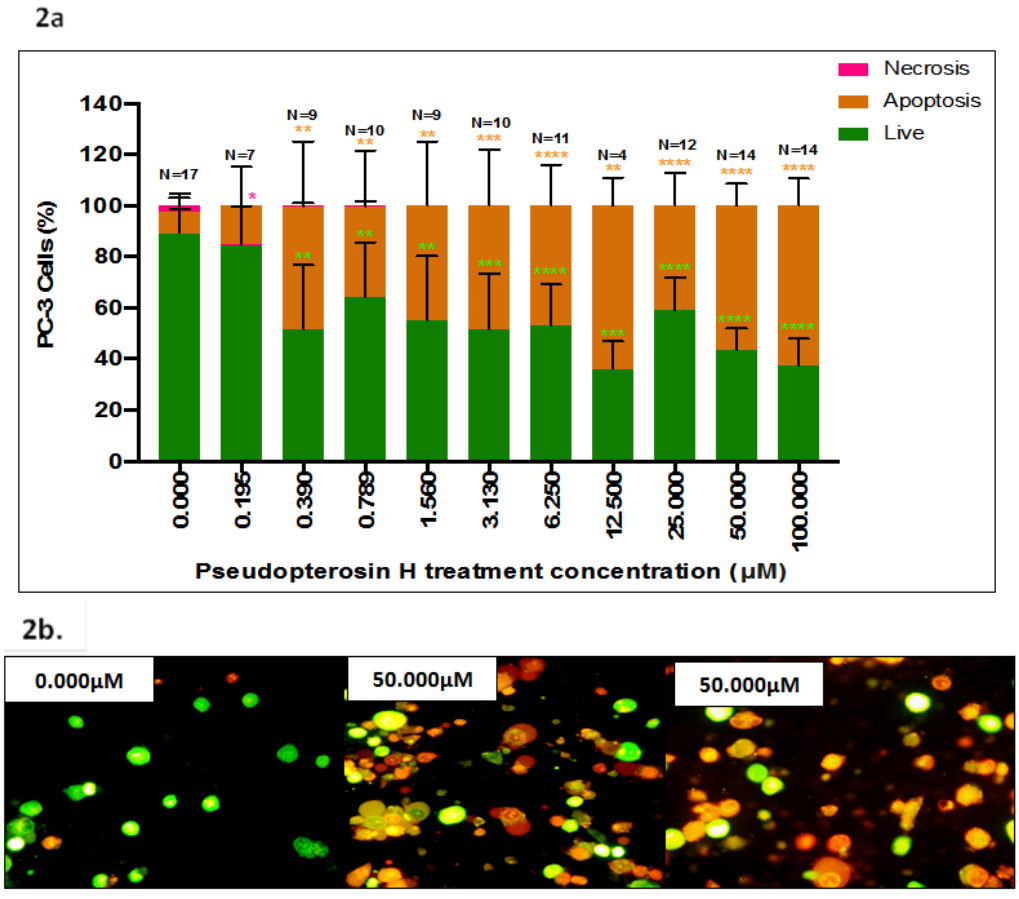

Figure 2 (2a) Percentage of live, apoptotic, and necrotic PC-3 cells after treatment with various concentrations of PsH (0.195µM-100.000µM). The percentage of PC-3 cells undergoing apoptosis increased (R^2 = 0.6563) and the percentage of live PC-3 cells decreased (R^2 = 0.6527) with an increasing PsH treatment concentration, relative to the negative control (0.000µM). PC-3 cells undergoing necrotic cell death were not observed at PsH treatment concentrations of 0.390µM- 100.000µM, and necrosis was independent of PsH treatment concentrations (R^2 = 0.06625). Data bars represent the mean percentage of live, apoptotic, and necrotic PC-3 cells, counted in a minimum of two frames at 40x magnification, in two independent trials (N=4 – N=17 microscope frames, amongst the two independent trials). Error bars represent ± standard deviation of the means amongst all trials. Statistical significance is denoted by a single (*) asterisk when p<0.0332, double asterisks (**) when p<0.0021, triple asterisks (***) when p<0.0002, and quadruple asterisks (****) when p<0.00001. **(2b)** Florescent microscope images (Nikon eclipse E600; 40x magnification) of PC-3 cells 48 hours after treatment with 0.000µM (negative control), 50.000µM PsH, and 100.000µM PsH. The green fluorescent emissions are indicative of live PC-3 cells, orange/brown of PC-3 cells undergoing apoptosis, and red (not pictured) of PC-3 cells undergoing necrosis.

Citation: Bowers Z, Caraballo D, Bentley A, et al. Therapeutic potential of Pseudopterosin H on a prostate cancer cell line. *J Cancer Prev Curr Res.* 2021;12(3):82–91. DOI: 10.15406/jcpcr.2021.12.00459

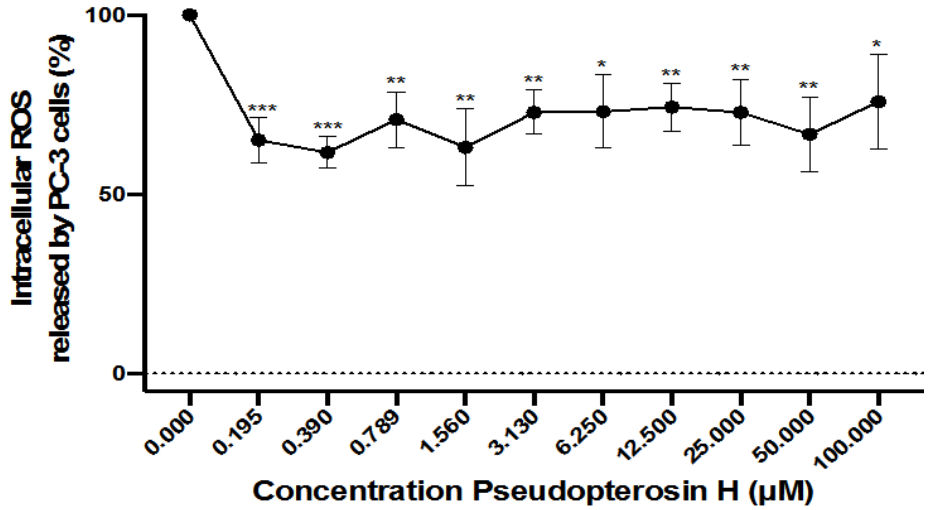

Figure 3 Percentage intracellular reactive oxygen species (ROS) released by PC-3 cells, at various PsH treatment concentrations (0.195µM-100.000µM). Treatment with PsH decreased the percentage of intracellular reactive oxygen species released by PC-3 cells after treatment, relative to that of the negative control (0.000µM). The downregulation of intracellular ROS by treatment with PsH was moderately dependent on treatment concentration ($R^2 = 0.677$). Data points represent the mean values of four independent experiments (N=3 96-well plates; 8 total wells per treatment concentration, per plate). Error bars represent ± standard deviation of the means amongst all trials. Statistical significance is denoted by a single (*) asterisk when $p<0.0332$, double asterisks (**) when $p<0.0021$, and triple asterisks (***) when $p<0.000$.

Discussion

Pseudopterosin H reduces PC-3 cell viability by inducing apoptosis

The anti-inflammatory and analgesic effects of Pseudopterosin compounds have been well studied throughout scientific literature.[1-8] Our study supports the growing evidence that these compounds may also possess therapeutic potential for the treatment, or prevention, of various cancers.[19,24,25,27,28,39] In this study, treatment with PsH effectively reduced PC-3 cell viability and altered cellular membrane integrity by inducing apoptosis as well as downregulated the level of intracellular reactive oxygen species (ROS) (Figure 1, 2, 3).

Treatment with PsH reduced PC-3 cell viability by significantly inducing apoptosis at concentrations of 0.390µM or greater, after 48 hours of treatment (Figure 2). Apoptosis is a strictly regulated homeostatic process that is critical for prevention of cancer progression and has been shown to enhance therapeutic success.[40,41] There was not a significant induction of necrosis in PC-3 cells treated with 0.390µM or greater of PsH, after 48 hours of treatment (Figure 2). Unlike apoptosis, necrosis is correlated with enhanced tumorigenesis due to the release of endogenous danger associated molecular patterns (DAMPS) that ultimately activate the key inflammatory pathway, NF-κβ.[15] Continuous activation of the NF-κβ pathway results in chronic inflammation and the overexpression of proinflammatory cytokines (i.e., interleukin 6 (IL-6) and interleukin 8 (IL-8)) which, in cancers, are associated with a poorer prognosis.[27] Although mCRPC resists apoptosis during ADT, the malignant cells retain the ability to undergo apoptosis and, therefore, compounds that induce apoptosis have potential pharmacological importance.[42] The results of the AO/EB fluorescence demonstrates that the decrease in PC-3 cell viability after treatment with PsH (Figure 1, 2) was likely due to the induction of apoptosis, despite a previous study suggesting that an increase in extracellular LDH is potentially indicative of necrosis.[43]

To our knowledge no scientific literature has been published on the effects of PsH on the PC-3 prostate cancer cell line, however, there have been numerous other studies on the anti-cancer activity of structurally related Pseudopterosin compounds on various other malignant cell lines. In a study performed on the MDA-MB-231 breast cancer cell line, PsA-D were concluded to have IC_{50} values for cell viability of 32.2µM, after 48 hours of treatment.[28] Another study assessed the cytotoxicity of PsP, PsQ, PsU, PsV, PsW to three cell lines (MCF-7, breast cancer; NCI-H460, non-small-cell lung cancer; SF-268, central nervous system) and demonstrated PsQ lacked cytotoxic effects across all cell lines, but PsP was highly cytotoxic (GI_{50} 1.7-5.8µM), as well as PsU and PsV (GI_{50} 20-100µM).[24] Additionally, the chemosensitivity of four malignant cell lines (HeLa, cervical cancer; PC-3, prostate cancer; HCT116, colorectal cancer; MCF-7, breast cancer) and one non-malignant (BJ, fibroblasts) cell line to treatment with PsG, PsP, PsQ, PsS, PsT, PsU, 3-*O*-acetyl-PsU, *seco*-PsJ and *seco*-PsK was determined.[25] This study concluded that PsG and PsQ were the most active compounds across all cell lines (GI_{50} 5.8-12.0µM), after 48 hours of treatment; PsG had a GI_{50} value of 8.83µM and PsQ of 7.81µM, on the PC-3 cell line.[25] PC-3 cell viability was less than 50% at PsH treatment concentrations of 25.000µM or greater, after 48 hours of treatment, relative to the negative control (0.000µM, 100%) (Figure 1). Treatment with PsH also caused an approximate 50-70% increase in cytotoxicity across all experimental concentrations after 48 hours of treatment, relative to the negative control (0.000µM, 0%) (Figure 1). The suggestive potency of PsH to PC-3 cells parallels these previous studies on structurally related Pseudopterosin compounds and various different malignant cell lines. However, due to the structural differences between Pseudopterosin compounds (glycosylation position, aglycone stereochemistry, and carbon skeleton) as well as differences in disease pathology and pathophysiology, no conclusive comparison of relative potency can be made.[24-28,38] Furthermore, it has been demonstrated that PsG, PsP, PsQ, PsS, PsT, PsU, 3-*O*-acetyl-PsU, *seco*-PsJ and *seco*-PsK are not selectively cytotoxic to malignant cell lines as they exhibited similar cytotoxic effects in the non-malignant cell line.[25] In regard to PsH, additional studies will need to be conducted on non-malignant cell lines to determine if PsH is selectively cytotoxic to PC-3 cells.

Citation: Bowers Z, Caraballo D, Bentley A, et al. Therapeutic potential of Pseudopterosin H on a prostate cancer cell line. *J Cancer Prev Curr Res.* 2021;12(3):82–91. DOI: 10.15406/jcpcr.2021.12.00459

Pseudopterosin H downregulates intracellular reactive oxygen species concentration in PC-3 cells, potentially through non-scavenging (indirect reduction of free radicals) activity

Treatment with PsH downregulated the concentration of intracellular reactive oxygen species (ROS) in PC-3 cells by approximately 25-39%, compared to that of the negative control (100.000%, 0.000µM) (Figure 3). Although low concentrations of ROS are necessary for homeostatic function of cellular signaling and generated during aerobic respiration, a hallmark of cancer is a sustained increase in ROS production caused by altered antioxidant defense enzymes and cellular metabolism.[44] Oxidative stress, resulting from increased non-homeostatic concentrations of ROS, is known to contribute to the progression of cancers through damaging intracellular components including DNA, lipids, and proteins.[30,45] The downregulation of ROS after treatment with PsH potentially arises from the compound altering the activity of ROS generating enzymes, such as NADPH oxidase (NOX), or indirectly through inhibiting the activation of the pro-inflammatory pathway, NF-κβ.[19,28,44]

NOX generates ROS by catalyzing NADPH and oxygen (O_2) to form the free radical ROS molecule, superoxide anion (O^-_2).[46] A previous study on the PC-3, LNCaP, and DU-145 prostate cancer cell lines demonstrated that NOX inhibition, through the use of diphenyliodonium, selectively inhibited the generation of ROS and resulted in decreased proliferation in all cell lines.[44] Numerous studies on Pseudopterosin compounds, however, suggest that the downregulation of ROS is most likely attributed to the compound affecting the activation of the NF-κβ pathway.[19,28] Increased ROS generation is correlated with activation of the NF-κβ pathway because activation of the NF-κβ pathway results in the expression, and secretion, of proinflammatory cytokines (i.e., IL-6 and IL-8).[27] An increase in intracellular concentrations of ROS (i.e., superoxide anions (O^-_2) and hydrogen peroxide (H_2O_2)) can then occur due to the promotion of acute and chronic inflammation through these proinflammatory cytokines, which is ultimately contributes to oncogenic transformation.[44] In studies performed on the MDA-MB-231 breast cancer cell line and THP-1 monocytic leukemia cells, treatment with PsA-D blocked activation of the NF-κβ pathway by inhibiting the phosphorylation of p65 and Iκβ (inhibitor of κβ).[19,28] An additional plausible reason for the downregulation of ROS after treatment with PsH could be, at least partially, attributed to the cytotoxicity of PsH to the PC-3 cells.

It is unlikely that PsH downregulated ROS through direct free radical scavenging activity as Pseudopterosin compounds, including PsH, have been shown to not possess their own antioxidant capabilities.[36,47] Additionally, the NBT assay provides insight into the effects of treatment on superoxide dismutase (SOD) enzyme activity. SOD is an antioxidant enzyme that catalyzes two superoxide anions (O^-_2) into oxygen (O_2) and hydrogen peroxide (H_2O_2).[48,49] The PC-3, LNCaP, and DU-145 cell lines have been shown to possess altered SOD enzyme function which promotes cell survival under oxidative stress.[44] It is unlikely that treatment with PsH altered SOD enzyme function because inhibition or reduction in SOD activity would have resulted in an upregulation of ROS.[48,49]

The ability of PsH to decrease intracellular ROS is prophylactically and therapeutically advantageous due to the critical role of oxidative stress in malignant cell survival and progression.[44] Although additional studies will need to be performed to determine the exact mechanism(s) involved, this study suggests PsH may alter prooxidant enzyme activity or inhibit NF-κβ pathway activation.

Materials and methods

Pseudopterosin H stock solution

The marine natural product, Pseudopterosin H, was isolated from the marine gorgonian octocoral *Pseudopterogorgia elisabethae*. Pseudopterosin H was dissolved in pure dimethyl sulfoxide (DMSO; 100%) to obtain a stock solution concentration of 100.000mM. DMSO concentration did not exceed 0.5% of the stock solution. The stock solution was then stored in the absence of light at 4°C, until experimental use.

Pseudopterosin H working solution and drug preparation

Methods: Pseudopterosin H stock solution (100.000mM) was diluted with RPMI 1640 media (Sigma Scientific, St. Louis, MO) to obtain a 100.000µM working solution. The working solution was temporarily stored in a 50ml conical tube wrapped in aluminum foil to avoid contact with laboratory lighting. Treatment concentrations were then prepared in a 96-well plate by serially diluting the 100.000µM working solution with RPMI 1640 media (Sigma Scientific, St. Louis, MO) to obtain Pseudopterosin H concentrations of 50.000µM-0.1953µM. The 10 Pseudopterosin H treatment concentrations (100.000µM-0.1953µM) were utilized throughout the study.

Calculations: To achieve dilution of the 100.000mM stock solution to a 100.000µM working solution, the equations (1, 2) were used; Volume (**V1**) of 100.000mM stock solution (**C1**) needed to obtain a final concentration of 100.000µM (**C2**) in a certain volume of RPMI 1640 media (**V2**) and the total volume (**total V**) of RPMI 1640 media needed for the dilution of the stock solution.

$$C1V1 = C2V2 \quad (1)$$

$$total\,V = V2 - V1 \quad (2)$$

PC-3 cell culture

The PC-3 prostate cancer cell line was purchased from the American Type Culture Collection (ATCC, Manassas, VA). The PC-3 cells were cultured and maintained in RPMI 1640 media supplemented with 15mM HEPES, 100µl/ml penicillin (1%), 100µg/ml streptomycin, 10% fetal bovine serum, and 100µg/ml L-glutamine (Sigma Scientific, St. Louis, MO). The cultured PC-3 cells were incubated (37°C, 5% CO_2) for 48 hours. After 48 hours of incubation, the cells were thoroughly dissociated and subjected to the Trypan Blue Exclusion assay (*Trypan Blue Exclusion Assay*). After, 100µl of the cell culture suspension was seeded into each well of the 96-well plate(s) to achieve a cellular density of $2.0x10^4$ per well.

Trypan blue exclusion assay

Purpose: The Trypan Blue exclusion assay was performed to establish an approximate cellular density of $2.0x10^4$ cells per well and assess cell viability before treatment. Cellular density and cell viability were determined using cellular membrane staining patterns. Live cells remain unstained due to their intact cellular membrane which is impermeable to the trypan blue dye, and dead cells stain dark blue due to their compromised cellular membrane, which is permeable to the trypan blue dye.[50]

Method: At the log phase of growth and 80-90% confluence (48 hours incubation; 37°C, 5% CO_2), cultured PC-3 cells were thoroughly dissociated and subjected to the Trypan Blue exclusion assay. 100µl of the PC-3 cell culture suspension was pipetted into a micro-centrifuge tube and 10µl of the trypan blue solution was added to the

Citation: Bowers Z, Caraballo D, Bentley A, et al. Therapeutic potential of Pseudopterosin H on a prostate cancer cell line. *J Cancer Prev Curr Res.* 2021;12(3):82–91. DOI: 10.15406/jcpcr.2021.12.00459

cell culture suspension using a micropipette. Through capillary action of the micropipette tip, one drop of the cell culture suspension and trypan blue solution mixture was then transferred to a two-chamber hemocytometer. Under a light microscope (Olympus BH2; 200x) the number of stained (dead) and unstained (live) cells were summed in a minimum of five separate squares (12 grids per square) of the two-chamber hemocytometer.

Calculations: The PC-3 cell culture viability percentage (equation 3), average number of viable cells per ml **(**equation 4**)**, and volume of cell culture suspension (V1; equation 5) needed for an approximate average density of $2x10^4$ cells per well (C2V2; equation 6), per 96-well plate(s) (equations 7), was determined using the following equations:

$$\%\ Viability = \left[\left(total\ live\ cells\right) / \left(total\ live\ cells + total\ dead\ cells\right)\right] x100 \quad (3)$$

$$Average\ number\ of\ viable\ cells = \left(total\ number\ of\ live\right) / \left(total\ number\ of\ squares\ counted\right) \quad (4)$$

$$Dilution\ factor\ \left(DF\right) = \left(volume\ cell\ suspension + volume\ trypan\ blue\ solution\right) / \left(volume\ cell\ suspension\right) \quad (5)$$

$$Concentration\ of\ cells\ in\ the\ suspension\ \left(C1\right) = \left(average\ number\ of\ viable\ cells\ /\ ml\right)\ \left(DF\right)\ \left(10\ \hat{}\ 4\ cells\ /\ ml\right) \quad (6)$$

$$C1V1 = C2V2 \quad (7)$$

PC-3 cell treatment

The PC-3 cells seeded in each 96-well plate were incubated for an additional 24 hours (37°C, 5% CO_2) to allow adherence (80-90% cell viability at a density of approximately $2.0x10^4$ cells per well). After 24 hours of incubation, the cell culture media was aspirated from each well and 100µl of each Pseudopterosin H treatment concentration (10 treatment concentrations; 100.000µM-0.1953µM) (*Pseudopterosin H Working Solution and Drug Preparation*) was pipetted into individual columns of the 96-well plate(s); One column per treatment concentration, 8 individual wells per column. Two columns of each 96-well plate were utilized as the control columns (Negative control, 0.000µM; Blank, RPMI 1640 media without cell culture). The treated cells were then incubated (37°C, 5% CO_2) for an additional 48 hours before performing the assay and fluorescent staining experiments.

MTT tetrazolium assay

Purpose: The MTT tetrazolium assay was performed to assess the viability of the PC-3 cells after treatment (37°C, 5% CO_2) with Pseudopterosin H. The yellow MTT (3-[4,5-dimethylthiazolyl-2,5-diphenyletrazolium bromide) tetrazolium salts are reduced into an insoluble purple formazan precipitate through the metabolic activity of dehydrogenase enzymes in live cells.[51,52] Metabolically inactive (dead) cells are unable to reduce MTT tetrazolium salts.[51,52] Cell viability is therefore directly proportional to the formazan precipitate present in the supernatant fluid, and quantified through spectrophotometric means.[51,52]

Method: After 48 hours of treatment (*PC-3 Cell Treatment* protocol***)***, 20µl of MTT reagent was pipetted into each well of the 96-well plate(s). The 96-well plate(s) were then incubated (37°C, 5% CO_2) with the MTT reagent until the purple formazan precipitate was visible (2-4 hours). The intracellular formazan was solubilized through the addition of 50µl of pure DSMO to each well of the 96-well plate(s). After the addition of DMSO, the 96-well plate(s) were incubated (37°C, 5% CO_2) for 30 minutes to 1 hour. The formazan product present in the supernatant fluid was then quantified using a BioTek microplate reader (BioTek ELx800; BioTek, Vermont, USA) to collect absorbance readings at 570nm. The resulting absorbance reading values were reported as a measure of live cells after treatment. Cell viability was calculated, amongst all trials (N=4 plates; 8 total wells per treatment concentration or negative control, per plate), as a percentage relative to the negative control (0.000µM) and graphed against treatment concentration.

Calculations: The 570nm absorbance values were averaged amongst each of the 10 treatment concentration groups ($\mathbf{T}_{570}$), negative control group ($\mathbf{NC}_{570}$), and blank group ($\mathbf{B}_{570}$) (8 individual wells per treatment or control group, per 96-well plate). The averaged blank ($\mathbf{B}_{570}$) absorbance value was then subtracted from the averaged absorbance values of each treatment concentration group **(**$\mathbf{T}_{570}{}^{*}$**)** and the negative control group ($\mathbf{NC}_{570}{}^{*}$) (equation 8). The treatment and negative control group values, calculated in equation (8), were then averaged amongst all plates at all trials (N=4 96-well plates; 8 total wells per treatment concentration, per plate) and the percentage of PC-3 cell viability after treatment, relative to the negative control ($\mathbf{NC}_{570}{}^{*}$), was determined (equation 9):[53]

$$\%\ Cell\ Viability = \left[\left(T_{570}{}^{*}\mathbf{or}NC_{570}{}^{*}\right) / \left(NC_{570}{}^{*}\right) x100\right] \quad (8)$$

$$\%\ Cell\ Viability = \left[\left(T_{570}{}^{*}\mathbf{or}NC_{570}{}^{*}\right) / \left(NC_{570}{}^{*}\right) x100\right] \quad (9)$$

Statistical analysis: An unpaired t-test was performed to determine if there was a statistically significant difference between the percentage of PC-3 cell viability, at the various experimental treatment group concentrations (10), and the negative control (0.000µM) (Graphpad Prism8, San Diego, USA). A linear regression model (95% confidence interval when X=0, Y=0; mean y values at each concentration point) was used to assess the fit of the trend line between the percentage of PC-3 cell viability and Pseudopterosin H treatment concentration (Graphpad Prism8, San Diego, USA). $P \leq 0.05$ was considered statistically significant.

Lactate dehydrogenase (LDH) cytotoxicity assay

Purpose: The Lactate Dehydrogenase (LDH) assay was performed to assess the cytotoxicity of treatment with Pseudopterosin H to PC-3 cells. LDH is a cytosolic enzyme that catalyzes an interconversion of pyruvate to lactate by reducing NAD^+ to NADH in most metabolically active cells.[43,54,55] Due to the cytosolic nature of the enzyme, drug cytotoxicity can be determined by the extracellular accumulation of LDH caused by a loss of cellular membrane integrity.[43,48,54,55] LDH present in the supernatant fluid reduces the assay's tetrazolium salts to a red formazan product which is proportional to cytotoxicity and quantified through spectrophotometric means.[48]

Method: After 48 hours of treatment (*PC-3 Cell Treatment* protocol***)***, 50.000µl of the supernatant fluid from each treatment and two negative control groups, was transferred into a new 96-well plate; This 96-well plate was used to carry out the LDH experiment. The LDH reaction mixture was prepared according to manufacturer protocols.[51] The spontaneous LDH activity control (3 total wells per

96-well plate) was prepared through the addition of 10µL of ultrapure water to the supernatant fluid from the negative control (0.000µM). The maximum LDH activity control (3 wells per 96-well plate) was prepared through the addition of 10.000ul 10x lysis buffer to the supernatant fluid from the negative control (0.000µM). Next, 50µl of the LDH reaction mixture was pipetted into each sample and control well. The LDH reaction mixture was then mixed with the contents of each well by gently tapping the plate. After mixing, the 96-well plate was incubated, in the dark, at room temperature (25°C), for 30 minutes. Following incubation, 50µL of stop solution was pipetted into each sample well in order to stop the reaction. The SpLDH and MxLDH controls were corrected to assure all wells contained a total volume of 150µl. Formazan present in the supernatant fluid was quantified through absorbance readings at 490nm and 630nm using a BioTek microplate reader (BioTek ELx800; BioTek, Vermont, USA). Cytotoxicity was calculated, amongst all trials (N=2 96-well plates; 8 total wells per treatment concentration, per plate), as a percentage relative to the negative control (0.000µM) and graphed against treatment concentration.

Calculations: The 490nm and 630nm absorbance values were individually averaged amongst each of the 10 treatment concentration groups (**T**) (8 individual wells per treatment group, per 96-well plate), negative control group (**NC**) (8 individual wells per control group per 96-well plate), maximum LDH control group (**MxLDH**) (3 individual wells per 96-well plate), and spontaneous LDH control group (**SpLDH**) (3 individual wells per 96-well plate). The averaged 490nm absorbance values were then subtracted from the corresponding averaged 630nm absorbance values for each group (equation 10). The new spontaneous LDH control (**SpLDH***) value was subtracted from each of the ten treatment concentration groups (**T***), negative control group (**NC***), and maximum LDH control group (**MxLDH***) (equation 11). The treatment, negative control, and maximum LDH control group values, calculated in equation **(**11**)**, were then averaged amongst all plates at all trials (N=2 96-well plates; 8 total wells per treatment concentration or negative control, per plate) and the percentage of PC-3 cell cytotoxicity after treatment (**T****), relative to the difference between the maximum LDH control (**MxLDH******)** and negative control (**NC****), was determined (equation 12):

$$\left(T_{490}-T_{630}\right)=T^{*},\left(NC_{490}-NC_{630}\right)=NC^{*},\left(MxLDH_{490}-MxLDH_{630}\right)=MxLDH^{*},\ \textbf{or}\left(SpLDH_{490}-SpLDH_{630}\right)=SpLDH^{*} \quad (10)$$

$$\left(T^{*}-SpLDH^{*}\right)=T^{**},\left(NC^{*}-SpLDH^{*}\right)=NC^{**},\textbf{or}\left(MxLDH^{*}-SpLDH^{*}\right)=MxLDH^{**} \quad (11)$$

$$\%\ Cytotoxicity=\left[\left(T^{**}-NC^{**}\right)/\left(MxLDH^{**}-NC^{**}\right)x100\right] \quad (12)$$

Statistical analysis: An unpaired t-test was used to determine if there was a statistically significant difference between the percentage of PC-3 cell cytotoxicity, at the various experimental treatment group concentrations (10), and the negative control (0.000µM) (Graphpad Prism8, San Diego, USA). A linear regression model (95% confidence interval when X=0, Y=0; mean y values at each concentration point) was used to assess the fit of the trend line between the percentage of PC-3 cell cytotoxicity and Pseudopterosin H treatment concentration (Graphpad Prism8, San Diego, USA). P≤0.05 was considered statistically significant.

Nitroblue Tetrazolium (NBT) Assay

Purpose: The Nitroblue Tetrazolium (NBT) assay was performed to assess the concentration of intracellular reactive oxygen species (ROS) produced by PC-3 cells after treatment with Pseudopterosin H, as well as evaluate superoxide dismutase (SOD) enzyme activity. In malignant prostate cancer cells oxidative stress, caused by a redox imbalance of ROS, is correlated with tumorigenesis and plays a vital role in transformation to aggressive androgen insensitive phenotypes.[45,48-50,56-60] SOD enzyme activity is of further interest due to the enzyme's activity in antioxidant defense. The SOD enzyme functions by catalyzing two superoxide anions (O_2^-) into an oxygen (O_2) and hydrogen peroxide (H_2O_2).[48,49] If inhibited, this enzyme would result in the upregulation of ROS.[48,49] Superoxide anions (i.e., ROS) reduce the NBT dye to NBT-diformazan. Inhibited SOD enzyme activity (acting as an antioxidant defense against superoxide anion) would, therefore, cause a decrease in quantifiable NBT-diformazan product. Due to this, the spectrophotometrically quantified NBT-diformazan product in the supernatant fluid is directly proportional to the concentration of intracellular ROS, and indirectly proportional to SOD enzyme activity.[50,51]

Method: After 48 hours of treatment (*PC-3 Cell Treatment* protocol*)*, 20µl of NBT solution (1mg/ml) was pipetted into each well of the 96-well plate. The 96-well plate was then incubated (37°C, 5% CO_2) for 4 hours. After incubation, the cellular membranes were lysed with pure DMSO in order to release the intracellularly accumulated NBT-diformazan product. The 96-well plate now containing DMSO was gently mixed using laboratory shaker before absorbance readings were taken. The amount of NBT-diformazan present in the supernatant fluid was quantified through absorbance readings at 490nm using a BioTek microplate reader (BioTek ELx800; BioTek, Vermont, USA). Intracellular ROS released by treatment was calculated, amongst all trials (N=3 plates; 8 total wells per treatment concentration, per plate; 16 total wells per negative control, per plate), as a percentage relative to the negative control (0.000µM) and graphed against treatment concentration.

Calculations: The 490nm absorbance values were averaged amongst each of the 10 treatment concentration groups ($\mathbf{T_{490}}$) and negative control group ($\mathbf{NC_{490}}$) (8 individual wells per treatment group, per 96-well plate; 16 individual wells per negative control group, per 96-well plate). The treatment ($\mathbf{T_{490}}$) and negative control ($\mathbf{NC_{490}}$) group values were then averaged amongst all plates at all trials (N=3 plates; 8 total wells per treatment concentration, per plate; 16 total wells per negative control, per plate) and the percentage of intracellular ROS released by PC-3 cells after treatment, relative to the negative control ($\mathbf{NC_{490}}$), was determined (equation 13):

$$\%ROS=\left[\left(T_{490}\ /\ NC_{490}\right)x100\right] \quad (13)$$

Statistical analysis: An unpaired t-test was used to determine if there was a statistically significant difference between the percentage of intracellular ROS released by PC-3 cells, at the various experimental treatment group concentrations (10), and the negative control (0.000µM) (Graphpad Prism8, San Diego, USA). A linear regression model (95% confidence interval when X=0, Y=0; mean y values at each concentration point) was used to assess the fit of the trend line between the percentage of intracellular ROS released by PC-3 cells and Pseudopterosin H treatment concentration (Graphpad Prism8, San Diego, USA). P≤0.05 was considered statistically significant.

Dual acridine orange/ethidium bromide (AO/EB) fluorescence

Purpose: AO/EB fluorescence was used to determine if the mode of PC-3 cellular death, after treatment with Pseudopterosin H, was apoptotic or necrotic. AO/EB fluorescence uses differential fluorescent emissions to differentiate live, apoptotic, or necrotic cells; AO causes both viable and nonviable cell nuclei to fluoresce green, while EB causes nonviable cell nuclei to fluoresce red.[49,50,61-64] A green, red, or orange/brown fluorescent emission is indicative of live cells, cells undergoing necrosis, or cells undergoing apoptosis, respectively.[49,56] Apoptosis is a necessary homeostatic process that is strictly regulated by caspase enzyme activation, and, in cancers, is critical for preventing cancer progression as well as enhancing therapeutic success.[65] Necrosis, unlike apoptosis, is unregulated and causes inflammation due to the release of endogenous danger associated molecular patterns (DAMPS).[40] In malignant tumors, chronic inflammation is associated with tumor progression, and it has been suggested that cancer therapies that induce apoptosis (non-inflammatory death process) may be superior to therapies that induce necrosis (inflammatory death process)).[40,60]

Method: After 48 hours of treatment (*PC-3 Cell Treatment* protocol), adhered PC-3 cells were dislodged and the supernatant fluid containing the cells was pipetted into microcentrifuge tubes that corresponded to the treatment or negative control groups. The supernatant was then centrifuged for 5 minutes at 3000 RPM. After centrifugation, the supernatant was discarded, and the cell pellet broken with 1ml PBS. This process (5 minutes centrifugation at 3000 RPM, removal of the supernatant, and breaking of the cell pellet) was repeated an additional three times. The AO and EB solutions were prepared as followed: 1mg of acridine orange (AO) per 10ml of PBS and 1mg of ethidium bromide (EB) per 10ml of PBS. 25µl of EB and 75µl of AO solutions were then combined in a separate microcentrifuge tube and vigorously mixed using a micropipette. After the fourth centrifugation process, the supernatant fluid was discarded for a final time and 25µl of the AO/EB solution was added to the remaining cell pellets, then vigorously mixed with a micropipette. Labeled microscope slides for each of the 10 treatment groups and negative control group, was prepared. Once prepared, 20µl of the PC-3 cell and AO/EB solution mixture was transferred onto each slide and covered with a coverslip. The microscope slides were analyzed under the fluorescent microscope (Nikon eclipse E600) with band pass filter at a magnification of 40x. Live, apoptotic, and necrotic cells after treatment were calculated, amongst all trials (N=4–N=17 microscope frames per treatment concentration group or negative control group, amongst two independent trials), as a percentage relative to the negative control (0.000µM) and graphed against treatment concentration.

Calculations: The fraction of live (**L**), apoptotic (**A**), or necrotic (**N**), PC-3 cells in each Pseudopterosin H treatment group (10), and negative control group, were calculated by counting the number of each cell type in each microscope frame (minimum of 2 frames per trial per treatment concentration or negative control group). Once each individual cell type was counted, the fraction of live (**L**), apoptotic (**A**), or necrotic (**N**) cells within the microscope field was calculated. These cell type fractions were then averaged amongst all microscope frames for each treatment concentration or control group, amongst the two independent trials (N=4–N=17 microscope frames per treatment concentration or negative control, amongst two independent trials). The overall percentage of live cells**,** apoptotic cells, and necrotic cells, amongst all trials, per treatment concentration (10) or negative control, was calculated using the following equations (equations 14-16):

$$\%\ Live\ cells = \left[L / \left(L + A + N \right) x100 \right] \quad (14)$$

$$\%\ Apoptosis = \left[A / \left(L + A + N \right) x100 \right] \quad (15)$$

$$\%\ Necrosis = \left[N / \left(L + A + N \right) x100 \right] \quad (16)$$

Statistical analysis: An unpaired t-test was used to determine if there was a statistically significant difference between the percentage of live, apoptotic, or necrotic cells PC-3 cells, at the various experimental treatment concentration groups (10), and the negative control 0.000µM) (Graphpad Prism8, San Diego, USA). A linear regression model (95% confidence interval when X=0, Y=0; mean y values at each concentration point) was used to assess the fit of the trend line between the percentage of live, apoptotic, or necrotic cells PC-3 cells and Pseudopterosin H treatment concentration (Graphpad Prism8, San Diego, USA). $P \leq 0.05$ was considered statistically significant.

Conclusion

The results of our study demonstrate that PsH reduces PC-3 cell viability by inducing apoptosis and downregulates ROS. The downregulation of ROS may arise from PsH directly affecting prooxidant enzyme function or indirectly through inhibition of the pro-inflammatory pathway, NF-κβ. Although the exact mechanisms of action remain unclear, PsH exhibits potentially advantageous pharmacological characteristics for the treatment of prostate cancer.

Acknowledgments

None.

Conflicts of interest

Authors declare that there is no conflict of interest.

References

1. Siegel RL, Miller KD, Fuchs HE, et al. Cancer Statistics, 2021. *CA: a Cancer Journal for Clinicians*. 2021;71(1):7–33.
2. Miller KD, Nogueira L, Mariotto AB, et al. Cancer treatment and survivorship statistics, 2019. *CA: a Cancer Journal for Clinicians*. 2019;69(5):363–385.
3. Hankey BF, Feuer EJ, Clegg LX, et al. Cancer surveillance series: interpreting trends in prostate cancer-part I: evidence of the effects of screening in recent prostate cancer incidence, mortality, and survival rates. *Journal of the National Cancer Institute*. 1999;91(12):1017–1024.
4. *Cancer Facts & Figures 2020*. Atlanta, GA: American Cancer Society; 2020.
5. Dong L, Zieren RC, Xue W, et al. Metastatic prostate cancer remains incurable, why?. *Asian Journal of Urology*. 2019;6(1):26–41.
6. Wang G, Zhao D, Spring DJ, et al. Genetics and biology of prostate cancer. *Genes & Development*. 2018;32(17-18):1105–1140.
7. Deng Q, Tang DG. Androgen receptor and prostate cancer stem cells: biological mechanisms and clinical implications. *Endocrine-Related Cancer*. 2015;22(6):T209–T220.
8. Yuan Xin, Steven P Balk. Mechanisms mediating androgen receptor reactivation after castration. *Urologic Oncology.* 2009;27(1):36–41.
9. Davey RA, Grossmann M. Androgen receptor structure, function and biology: from bench to bedside. *The Clinical Biochemist Reviews*. 2016;37(1):3–15.

10. Rawla P. Epidemiology of prostate cancer. *World Journal of Oncology*. 2019;10(2):63–89.

11. Tai S, Sun Y, Squires JM, et al. PC3 is a cell line characteristic of prostatic small cell carcinoma. *The Prostate*. 2011;71(15):1668–1679.

12. Alves C, Silva J, Pinteus S, et al. From marine origin to therapeutics: The antitumor potential of marine algae-derived compounds. *Frontiers in Pharmacology*. 2018;9:777.

13. Li G, Lou HX. Strategies to diversify natural products for drug discovery. *Medicinal Research Reviews*. 2018;38(4):1255–1294.

14. Ruiz-Torres V, Encinar JA, Herranz-López M, et al. An updated review on marine anticancer compounds: The use of virtual screening for the discovery of small-molecule cancer drugs. *Molecules*. 2017;22(7):1037.

15. Mayer AM, Glaser KB, Cuevas C, et al. The odyssey of marine pharmaceuticals: a current pipeline perspective. *Trends in Pharmacological Sciences*. 2010;31(6):255–265.

16. Newland AM, Li JX, Wasco LE, et al. Brentuximab Vedotin: A CD 30-Directed Antibody-Cytotoxic Drug Conjugate. *Pharmacotherapy: The Journal of Human Pharmacology and Drug Therapy*. 2013;33(1):93–104.

17. Koski RR. Omega-3-acid ethyl esters (Lovaza) for severe hypertriglyceridemia. *Pharmacy and Therapeutics*. 2008;33(5):271–303.

18. Petersen LE, Kellermann MY, Schupp PJ. Secondary Metabolites of Marine Microbes: From Natural Products Chemistry to Chemical Ecology. In *YOUMARES 9-The Oceans: Our Research, Our Future*. Springer: Cham; 2020. 159–180 p.

19. Dyshlovoy S, Honecker F. Marine compounds and cancer: 2017 updates. *Mar Drugs*. 2018;16(2):41.

20. Pereira F. Have marine natural product drug discovery efforts been productive and how can we improve their efficiency?. *Expert Opin Drug Discov*. 2019;14(8):717–722.

21. Gerwick WH, Moore BS. Lessons from the past and charting the future of marine natural products drug discovery and chemical biology. *Chemistry & Biology*. 2012;19(1):85–98.

22. Malve H. Exploring the ocean for new drug developments: Marine pharmacology. *Journal of Pharmacy & Bioallied Sciences*. 2016;8(2):83–91.

23. Onumah N. A novel anti-inflammatory in treatment of acne vulgaris: the pseudopterosins. *Journal of Drugs in Dermatology.* 2013;12(10):1177–1179.

24. Rodríguez II, Shi YP, García OJ, et al. New Pseudopterosin and seco-Pseudopterosin Diterpene Glycosides from Two Colombian Isolates of Pseudopterogorgia e lisabethae and Their Diverse Biological Activities. *Journal of Natural Products*. 2004;67(10):1672–1680.

25. Correa H, Aristizabal F, Duque C, et al. Cytotoxic and antimicrobial activity of pseudopterosins and seco-pseudopterosins isolated from the octocoral Pseudopterogorgia elisabethae of San Andres and Providencia Islands (Southwest Caribbean Sea). *Marine Drugs*. 2011;9(3):334–343.

26. Duque C, Castellanos L, Tello E. Structure-Activity Relationship (SAR) Studies to Maximize the Activity of Compounds Isolated from Octocorals. *Corals in a Changing World*. 2018;271.

27. Sperlich J, Kerr R, Teusch N. The marine natural product pseudopterosin blocks cytokine release of triple-negative breast cancer and monocytic leukemia cells by inhibiting NF-κB signaling. *Marine drugs*. 2017;15(9):262.

28. Sperlich J, Teusch N. Pseudopterosin inhibits proliferation and 3D invasion in triple-negative breast cancer by agonizing glucocorticoid receptor alpha. *Molecules*. 2018;23(8):1992.

29. Look SA, Fenical W, Jacobs RS, et al. The pseudopterosins: anti-inflammatory and analgesic natural products from the sea whip Pseudopterogorgia elisabethae. *Proceedings of the National Academy of Sciences*. 1986;83(17):6238–6240.

30. Caplan SL, Zheng B, Dawson-Scully K, et al. Pseudopterosin A: Protection of synaptic function and potential as a neuromodulatory agent. *Marine Drugs*. 2016;14(3):55.

31. Ruoslahti E. How cancer spreads. *Scientific American*. 1996;275(3):72–77.

32. McConnell OJ, Longley RE, Koehn FE. The discovery of marine natural products with therapeutic potential. *Biotechnology (Reading, Mass.)*. 1994;26:109–174.

33. Berrué F, McCulloch MW, Kerr RG. Marine diterpene glycosides. *Bioorganic & Medicinal Chemistry*. 2011;19(22):6702–6719.

34. Kerr RG, Kohl AC, Ferns TA. Elucidation of the biosynthetic origin of the anti-inflammatory pseudopterosins. *Journal of Industrial Microbiology and Biotechnology*. 2006;33(7):532–538.

35. Thornton RS, Kerr RG. Induction of pseudopterosin biosynthesis in the gorgonian Pseudopterogorgia elisabethae. *Journal of Chemical Ecology*. 2002;28(10):2083–2090.

36. Mydlarz LD, Jacobs RS, Boehnlein J, et al. Pseudopterosin biosynthesis in Symbiodinium sp., the dinoflagellate symbiont of Pseudopterogorgia elisabethae. *Chemistry & Biology*. 2003;10(11):1051–1056.

37. Zhong W, Moya C, Jacobs RS, et al. Synthesis and an evaluation of the bioactivity of the C-glycoside of pseudopterosin A methyl ether. *The Journal of Organic Chemistry*. 2008;73(18):7011–7016.

38. Look SA, Fenical W, Jacobs RS, et al. The pseudopterosins: anti-inflammatory and analgesic natural products from the sea whip Pseudopterogorgia elisabethae. *Proceedings of the National Academy of Sciences*. 1986;(17):6238–6240.

39. Dyshlovoy SA, Honecker F. Marine Compounds and Cancer: Where Do We Stand? *Mar Drugs.* 2015;13(9):5657–5665.

40. Karsch-Bluman A, Feiglin A, Arbib E, et al. Tissue necrosis and its role in cancer progression. *Oncogene*. 2019;38(11):1920–1935.

41. Lowe SW, Lin AW. Apoptosis in cancer. *Carcinogenesis*. 2000;21(3):485–495.

42. Joo SS, Yoo YM. Melatonin induces apoptotic death in LNCaP cells via p38 and JNK pathways: therapeutic implications for prostate cancer. *Journal of Pineal Research*. 2009;47(1):8–14.

43. Chan FKM, Moriwaki K, De Rosa MJ. Detection of necrosis by release of lactate dehydrogenase activity. In *Immune Homeostasis*. Humana Press: Totowa, NJ; 2013. 65–70 p.

44. Khandrika L, Kumar B, Koul S, et al. Oxidative stress in prostate cancer. *Cancer Letters*. 2009;282(2):125–136.

45. Kumar B, Koul S, Khandrika L, et al. Oxidative stress is inherent in prostate cancer cells and is required for aggressive phenotype. *Cancer Research*. 2008;68(6):1777–1785.

46. Babior BM. NADPH oxidase. *Current Opinion in Immunology*. 2004;16(1):42–47.

47. Jacobs R, Mydlarz L, Moya C. *U.S. Patent Application No. 10/899,054*; 2005.

48. Famuyiwa TO. The Impact of PLGA Nanoparticle Delivered 3-Bromopyruvate and SC-514 on ABC Transporter Mediated Multidrug Resistance in Prostate Cancer Treatment. *The FASEB Journal*. 2018;32(Suppl 1):804–825.

49. Famuyiwa T, Boe A, Diaka K, et al. Vitamin C impact on genistein-induced cell death in prostate cancer. In *1st Electronic Conference on Molecular Science*. Multidisciplinary Digital Publishing Institute; 2015.

50. Famuyiwa TO. *Impact of vitamin C on genistein induced apoptosis on prostate cancer*. Florida Atlantic University; 2015.

51. Riss TL, Moravec RA, Niles AL, et al. Cell viability assays. In *Assay Guidance Manual [Internet]*. Eli Lilly & Company and the National Center for Advancing Translational Sciences; 2016.

Citation: Bowers Z, Caraballo D, Bentley A, et al. Therapeutic potential of Pseudopterosin H on a prostate cancer cell line. *J Cancer Prev Curr Res*. 2021;12(3):82–91. DOI: 10.15406/jcpcr.2021.12.00459

52. Huet O, Petit JM, Ratinaud MH, et al. NADH-dependent dehydrogenase activity estimation by flow cytometric analysis of 3-(4, 5-dimethylthiazolyl-2-yl)-2, 5-diphenyltetrazolium bromide (MTT) reduction. *Cytometry: The Journal of the International Society for Analytical Cytology*. 1992;13(5):532–539.

53. Famuyiwa TO, Jebelli J, Diaka JKK. Interaction between 3-Bromopyruvate and SC-514 in prostate cancer treatment. *J Cancer Prev Curr Res*. 2018;9(6):270–280.

54. Kaja S, Payne AJ, Naumchuk Y, et al. Quantification of lactate dehydrogenase for cell viability testing using cell lines and primary cultured astrocytes. *Current Protocols in Toxicology*. 2017;72(1):2–26.

55. Feng Y, Xiong Y, Qiao T, et al. Lactate dehydrogenase A: A key player in carcinogenesis and potential target in cancer therapy. *Cancer Medicine*. 2018;7(12):6124–6136.

56. Dal Berto M, Bica CG, de Sá GP, et al. The effect of superoxide anion and hydrogen peroxide imbalance on prostate cancer: An integrative in vivo and in vitro analysis. *Medical Oncology*. 2015;32(11):251.

57. Marchi S, Giorgi C, Suski JM, et al. Mitochondria-ros crosstalk in the control of cell death and aging. *Journal of Signal Transduction*. 2012;2012:329635.

58. Holl M, Koziel R, Schafer G, et al. ROS signaling by NADPH oxidase 5 modulates the proliferation and survival of prostate carcinoma cells. *Molecular Carcinogenesis*. 2016;55(1):27–39.

59. Panieri E, Santoro MM. ROS homeostasis and metabolism: a dangerous liason in cancer cells. *Cell Death & Disease*. 2016;7(6):e2253.

60. Lin CJ, Lee CC, Shih YL, et al. Inhibition of mitochondria-and endoplasmic reticulum stress-mediated autophagy augments temozolomide-induced apoptosis in glioma cells. *PloS One*. 2012;7(6):e38706.

61. Mironova EV, Evstratova AA, Antonov SM. A fluorescence vital assay for the recognition and quantification of excitotoxic cell death by necrosis and apoptosis using confocal microscopy on neurons in culture. *Journal of Neuroscience Methods*. 2007;163(1):1–8.

62. Singh AV, Xiao D, Lew KL, et al. Sulforaphane induces caspase-mediated apoptosis in cultured PC-3 human prostate cancer cells and retards growth of PC-3 xenografts in vivo. *Carcinogenesis*. 2004;25(1):83–90.

63. Kasibhatla S, Amarante-Mendes GP, Finucane D, et al. Acridine orange/ethidium bromide (AO/EB) staining to detect apoptosis. *Cold Spring Harbor Protocols*. 2006;(3):pdb-prot4493.

64. Liu K, Liu PC, Liu R, et al. Dual AO/EB staining to detect apoptosis in osteosarcoma cells compared with flow cytometry. *Medical Science Monitor Basic Research*. 2015;21:15–20.

65. Ichim G, Tait SW. A fate worse than death: apoptosis as an oncogenic process. *Nature Reviews Cancer*. 2016;16(8):539–548.

Citation: Bowers Z, Caraballo D, Bentley A, et al. Therapeutic potential of Pseudopterosin H on a prostate cancer cell line. *J Cancer Prev Curr Res*. 2021;12(3):82–91. DOI: 10.15406/jcpcr.2021.12.00459